NEOPLASIA
www.neoplasia.com

Volume 11 Number 6 June 2009 pp. 552–563 552

A Rationally Designed Histone Deacetylase Inhibitor with Distinct Antitumor Activity against Ovarian Cancer[1,2]

Ya-Ting Yang*[,3], Curt Balch[†,‡], Samuel K. Kulp*, Michael R. Mand[†], Kenneth P. Nephew[†,‡] and Ching-Shih Chen*

*Division of Medicinal Chemistry and Pharmacognosy, College of Pharmacy, The Ohio State University, Columbus, OH, USA; [†]Medical Sciences, Indiana University School of Medicine, Bloomington, IN, USA; [‡]Indiana University Cancer Center, Indianapolis, IN, USA

Abstract

Histone deacetylase inhibitors (HDACIs) are a class of antineoplastic agents previously demonstrating preclinical chemosensitizing activity against drug-resistant cancer cells and mouse xenografts. However, whereas clinical studies have shown efficacy against human hematologic malignancies, solid tumor trials have proved disappointing. We previously developed a novel HDACI, "OSU-HDAC42," and herein examine its activity against ovarian cancer cell lines and xenografts. OSU-HDAC42, (i) unlike most HDACIs, elicited a more than five-fold increase in G_2-phase cells, at 2.5 μM, with G_2 arrest followed by apoptosis; (ii) at 1.0 μM, completely repressed messenger RNA expression of the cell cycle progression gene *cdc2*; (iii) at low doses (0.25-1.0 μM for 24 hours), induced tumor cell epithelial differentiation, as evidenced by morphology changes and a more than five-fold up-regulation of epithelium-specific cytokeratins; (iv) potently abrogated the growth of numerous ovarian cancer cells, with IC_{50} values of 0.5 to 1.0 μM, whereas also remaining eight-fold less toxic (IC_{50} of 8.6 μM) to normal ovarian surface epithelial cells; and (v) chemosensitizated platinum-resistant mouse xenografts to cisplatin. Compared with the clinically approved HDACI suberoylanilide hydroxamic acid (vorinostat), 1.0 μM OSU-HDAC42 was more biochemically potent (i.e., enzyme-inhibitory), as suggested by greater gene up-regulation and acetylation of both histone and nonhistone proteins. In p53-dysfunctional cells, however, OSU-HDAC42 was two- to eight-fold less inductive of p53-regulated genes, whereas also having a two-fold higher IC_{50} than p53-functional cells, demonstrating some interaction with p53 tumor-suppressive cascades. These findings establish OSU-HDAC42 as a promising therapeutic agent for drug-resistant ovarian cancer and justify its further investigation.

Neoplasia (2009) 11, 552–563

Introduction

Ovarian cancer is the most lethal gynecological cancer in women. Whereas stage I disease has a 5-year survival rate of more than 93%, 75% of patients initially present with disseminated (stage III/IV) disease, for which survival falls to less than 25% [1]. Although surgical debulking, followed by platinum (e.g., cisplatin or carboplatin) and taxane regimens, provides responses to more than 70% of patients [2], more than 85% of those responders eventually relapse, at which point further therapy options are very limited [2]. Consequently, strategies aimed at resensitization would greatly reduce the mortality and human suffering of this devastating malignancy.

In the early 1970s, several compounds were discovered to elicit differentiation of Friend erythroleukemia cells; many of these were later demonstrated to enhance histone acetylation due to the inhibition of

Abbreviations: HDAC, histone deacetylase; HDACI, histone deacetylase inhibitor; SAHA, suberoylanilide hydroxamic acid; VPA, valproic acid; AE1/AE3, a mixture of two monoclonal antibodies (AE1 and AE3), with broad specificity against cytokeratins; NOSE, normal ovarian surface epithelial; PARP, poly(ADP) ribosylase polymerase

Address all correspondence to: Ching-Shih Chen, PhD, Division of Medicinal Chemistry, College of Pharmacy, The Ohio State University, 500 W 12th Ave, Columbus, OH 43210. E-mail: chen.844@osu.edu or Curt Balch, PhD, Medical Sciences Program, 300 Jordan Hall, 1001 E Third St, Indiana University, Bloomington, IN 47405. E-mail: rbalch@indiana.edu

[1]This work was supported by National Cancer Institute grants CA085289, CA113001 (to K.P.N.), and CA112250 (to C.-S.C.), an award from the Phi Beta Psi Sorority (to K.P.N.), and an award from Ovar'coming Together (Indianapolis, IN) (to C.B.).

[2]This article refers to supplementary materials, which are designated by Tables W1 and W2 and Figures W1 to W4 and are available online at www.neoplasia.com.

[3]Current address: Division of Immunology, The Scripps Research Institute, 10550 N Torrey Pines Rd, La Jolla, CA 92037.

Received 21 January 2009; Revised 10 March 2009; Accepted 11 March 2009

DOI 10.1593/neo.09204

histone deacetylase (HDAC) enzymes [3,4]. After further *in vitro* and animal testing, several of these, and other fortuitously discovered, compounds (or their derivatives) entered clinical trials [5,6]. These agents included suberoylanilide hydroxamic acid (SAHA, vorinostat), depsipeptide (FK228, romidepsin), MS-725 (SNDX-275), and valproic acid (VPA, divalproex), and SAHA has now been approved for cutaneous T-cell lymphoma [7]. Activity against solid tumors, however, has thus far been disappointing [8–10], and a recent phase 1 ovarian cancer clinical trial of SAHA demonstrated minimal patient benefit [11]. Whereas some recently examined (third-generation) HDAC inhibitors have been designed based on now-solved HDAC structures [12] (with the first structure, that of the HDAC-like protein, published in 1999) [13], most second-generation compounds currently in clinical trials (including SAHA, first reported in 1996) [14] were developed based on their capacity for inducing differentiation of erythroleukemia cells or antitumor activities in mice [14–17]. Consequently, despite their biological activity, it is possible that the enzyme-inhibitory activities of those widely studied (and likely clinically viable) HDACIs could yet be further improved [12].

To address these possibilities, we rationally designed a novel HDAC inhibitor (HDACI), designated "OSU-HDAC42," by tethering a short-chain fatty acid to a Zn^{2+}-chelating hydroxamate group, using a hydrophobic spacer for optimal interaction with the HDAC active site pocket [18]. Previously, OSU-HDAC42 (NSC-D736012; AR-42 Arno Therapeutics, Inc., Fairfield, NJ) was found to be more potent than SAHA against human prostate cancer cells and xenografts [19], in addition to completely abrogating tumor progression of a spontaneously occurring mouse model (TRAMP) of that malignancy [20]. In a similar preclinical study of human hepatocellular carcinoma, orally administrated OSU-HDAC42 suppressed xenograft tumor growth by more than 90% (compared with 66% by SAHA), whereas also being 85% repressive of further growth of preexisting tumors (i.e., developed before treatment) [21]. Mechanistically, OSU-HDAC42 was previously demonstrated to disrupt repressive protein phosphatase 1 interactions with HDACs 1 and 6, allowing protein phosphatase 1–mediated dephosphorylation (and thus inactivation) of the oncogenic signaling mediator Akt [22]. OSU-HDAC42 was also demonstrated to sensitize drug-resistant DU-145 prostate cancer cells to double-strand DNA breaking agents by enhancing acetylation (resulting in inhibition of DNA binding) of the DNA repair enzyme Ku70 [23]. Whereas the precise role of Ku70 in the repair of platinum-DNA adducts (*vs* double-strand breaks) remains controversial [24,25], the aforementioned study provided impetus for examining OSU-HDAC42 as a possible chemosensitizing agent for ovarian cancer (a disease that almost inevitably progresses to a platinum-resistant phenotype) [26].

On the basis of these findings, OSU-HDAC42 has now undergone extensive preclinical assessment within the Rapid Access to Intervention Development program of the National Cancer Institute, and was recently licensed to a biopharmaceutical company (Arno Therapeutics). Similar to most malignancies, advanced-stage ovarian cancer undergoes a number of epigenetic aberrations, including dysregulated HDAC expression [27,28]. In the current preclinical study, OSU-HDAC42 was found antiproliferative to both ovarian cancer cells and tumors, based on unique mechanisms of cytostasis, differentiation, and apoptosis, and in combination with cisplatin, OSU-HDAC42 significantly delayed growth of platinum-resistant tumors in mice. Whereas most HDACIs elicit cytostasis by G_1 arrest [5,29], OSU-HDAC42 likely elicits G_2 blockage through an atypical mechanism, that is, transcriptional repression of the cell cycle progression protein cdc2. In summary, OSU-HDAC42 represents a promising antineoplastic agent for advanced, drug-resistant ovarian cancer and warrants further investigation for the therapy for this highly destructive malignancy.

Materials and Methods

Reagents and HDAC Inhibitor Synthesis

Cisplatin for *in vitro* study was purchased from Sigma-Aldrich (St. Louis, MO) and dissolved in PBS at a stock concentration of 2 mM. For *in vivo* studies, a premanufactured saline solution of cisplatin (Novaplus, Irving, TX) was used. The HDACIs SAHA and OSU-HDAC42 were synthesized in our laboratory [18]. For *in vitro* studies, stock solutions were prepared in DMSO and diluted in culture medium for cell treatments. For *in vivo* studies, HDACIs were prepared as suspensions in vehicle (0.5% methylcellulose, 0.1% Tween 80, in sterile water). Antibodies against PI3K, PTEN, Akt, acetyl-H3, phospho-Ser^{473}-Akt, and cdc2 were purchased from Cell Signaling Technology (Danvers, MA), anti–histone H3 from Upstate (Lake Placid, NY), and antibodies against p21 and cyclin B1 from Santa Cruz Biotechnology (Santa Cruz, CA). Cell culture reagents were from Invitrogen (Carlsbad, CA) or HyClone (Logan, UT).

Cell Culture Studies

The $p53^{+/+}$ cisplatin-sensitive human ovarian cancer cell line A2780 was purchased from the European Collection Association of Cell Culture (Cambridge, United Kingdom), whereas the cisplatin-resistant cell lines CP70 (p53-mutant) and OVCAR10 (p53-functional) were kindly provided by Dr. T-H.M. Huang (Ohio State University). A2780, CP70, and OVCAR10 cells were cultured at 37°C, under 5% CO_2, in RPMI-1640 medium supplemented with 10% FBS and 2 mM L-glutamine. Primary normal ovarian surface epithelial (NOSE) cells were obtained from healthy women by gentle brushing of the ovarian surface, followed by short-term (two to four passages) expansion in culture, as previously described [30].

Dose-Response Studies of Normal Epithelial or Malignant Ovarian Cells

To assess cell viability, cells (5000/well in 96-well plates) were treated with various concentrations of OSU-HDAC42 (see figures), for 2 days, followed by analysis of MTT (TCI America, Portland, OR) tetrazolium salt metabolism [19], using six experimental replicates. That specific starting cell number (5000/well) was selected for the 48-hour incubation based on the assumption of subconfluency after three cell divisions or less (and thus approximately 40,000 cells/well), with 50,000 cells representing a confluent well of 0.3-cm^2 surface area (http://www.bdbiosciences.com). For NOSE cells (see previous paragraph), which divide substantially more slowly than transformed cells [31], 10,000 cells were seeded per well, with 5-day drug treatments. On the basis of the resultant A_{570} readings, IC_{50} values (i.e., drug dose requirements for 50% growth inhibition) were determined by Calcusyn (Biosoft, Cambridge, UK), using the "median-effect" method [32], or Prism 4, using sigmoidal dose (variable slope) curve fitting (GraphPad Software, San Diego, CA).

Western Blot Analysis

For immunoblot analysis, OSU-HDAC42–treated (48 hours, see figures) cells were lysed followed by protein isolation and quantification

(Bradford assay; Bio-Rad, Hercules, CA) and SDS-PAGE. Proteins were then transferred to nitrocellulose membranes and subjected to immunoblot analysis as previously described [19].

Semiquantitative or Fully Quantitative Reverse Transcription–Polymerase Chain Reaction Assessments of Gene Expression

For gene expression analysis, OSU-HDAC42–treated cells (see figures) were harvested, total RNA–extracted (RNeasy; Qiagen, Valencia, CA), reverse-transcribed using an iScript cDNA synthesis kit (Bio-Rad). After reverse transcription, cDNA was polymerase chain reaction (PCR)–amplified for specific gene transcripts, for 30 cycles, and analyzed on 2% agarose (semiquantitative analysis) or was mixed with a SYBR green–based PCR reaction mixture (Roche Applied Science, Indianapolis, IN) and analyzed for 45 cycles (fully quantitative analysis) using a LightCycler 2.0 real-time PCR instrument (Roche). Relative changes in transcript levels were determined by the $2^{(-\Delta\Delta Ct)}$ method [33] using *β-actin* or *E2F-1* as reference housekeeping genes. Gene-specific primer sequences are available upon request.

Cell Cycle Distribution Analyses

After various 48-hour drug treatments (see figures), cells (1×10^6) were harvested, and processed as previously described [21], with flow cytometry performed using a FACSCalibur (BD Biosciences, Franklin Lakes, NJ) instrument and data analysis using ModFit (Verity Software House, Topsham, ME). For sub-G_1 population analysis, both floating and adherent cells were collected.

Annexin V/Propidium Iodide Apoptosis Analysis

To quantify apoptosis, cells (2×10^5 per well in six-well plates) were treated for 48 hours with media or 0.5, 1.0, or 2.5 μM OSU-HDAC42. After drug treatments, both floating and adherent cells were collected, stained with a propidium iodide (PI)/annexin V–fluorescein solution (Invitrogen) for 15 minutes at room temperature in the dark, and flow cytometry was performed as described previously. For drug combination studies, cells were pretreated for 4 hours with OSU-HDAC42 (see text for doses) followed by media or 5, 10, or 25 μM cisplatin for 48 hours.

Cell Morphology and Cytokeratin Expression Analyses

To examine drug-induced ovarian cancer cell morphology changes, cells (2×10^5 per well in six-well plates) were treated for 24 hours with 0 to 2.5 μM OSU-HDAC42, followed by photography under phase-contrast magnification. For the assessment of epithelial differentiation, CP70 cells were grown on coverslips, treated with vehicle, 0.5, or 1.0 μM OSU-HDAC42 for 48 hours, and fixed with 4% paraformaldehyde for 20 minutes at 37°C. Fixed cells were then washed with PBS, blocked for 1 hour in PBS containing 1% FBS and 0.1% Triton X-100, and incubated with the monoclonal antibody (1:100 in PBS/0.1% BSA) cocktail AE1/AE3 (DakoCytomation, Carpinteria, CA), which recognizes most human cytokeratins [34], for 24 hours. Cells were then washed thrice with PBS, incubated with 3% H_2O_2 (in PBS) for 5 minutes to inactivate endogenous peroxidases, washed twice, and incubated with biotin-conjugated anti–mouse antibodies, followed by streptavidin-peroxidase. Finally, pan-cytokeratins were detected using a diaminobenzidine substrate kit (Vector Labs, Burlingame, CA).

For quantifying OSU-HDAC42–mediated CP70 epithelial differentiation, we performed flow cytometry again using AE1/AE3. Briefly, 48 hours OSU-HDAC42–treated cells were washed, fixed in 50% ethanol overnight (at −20°C), pelleted, PBS-washed, and permeabilized with PBS/0.1% Triton X-100 for 10 minutes at room temperature. After washing, cells were resuspended in 100 μl AE1/AE3 (1:100 in PBS/0.1% BSA) for 2 hours at room temperature on a rocker. After PBS washing of primary antibody, cells were stained (in the dark) with 100 μl of Alexa Fluor 488 goat anti–mouse IgG (Invitrogen; 1:200 in PBS/0.1% BSA) on a rocking platform for 2 hours at room temperature. Five hundred milliliters of PBS was then added to increase the volume for flow cytometric analysis (described previously).

In Vivo *Xenograft Drug Sensitivity Tumor Studies*

Mouse xenograft studies were carried out with strict adherence to protocols approved by the Institutional Animal Care and Use Committee of The Ohio State University. Female athymic nude mice (NCr-*nu/nu*, 5-7 weeks of age), obtained from the National Cancer Institute (Frederick, MD), were subcutaneously inoculated with 5×10^5 CP70 cells, in 0.1 ml of Matrigel (BD Biosciences; 50% [v/v] in serum-free medium), in the right dorsal flank. When individual tumors reached a volume of 100 mm^3, mice were randomized into eight groups (eight mice/group) for treatment with the following: 1) vehicle; 2) 6 mg/kg cisplatin every 6 days; 3) 25 mg/kg OSU-HDAC42 once daily; 4) 50 mg/kg OSU-HDAC42 every other day; 5) 50 mg/kg SAHA once daily; 6) 25 mg/kg OSU-HDAC42 once daily and 6 mg/kg cisplatin every 6 days; 7) 50 mg/kg OSU-HDAC42 every other day with 6 mg/kg cisplatin; and 8) 50 mg/kg SAHA once daily with 6 mg/kg cisplatin (Table W1). Vehicles used for *in vivo* studies were PBS (cisplatin) and 0.5% methylcellulose, 0.1% Tween 80, in sterile water (for HDACIs). Histone deacetylase inhibitor doses were based on an *in vivo* mouse SAHA study of prostate cancer xenografts [35], whereas the cisplatin dose was based on a previous ovarian cancer xenograft study [36]. Vehicle, OSU-HDAC42, and SAHA were each administered by oral gavage, and cisplatin was administered by intraperitoneal injection. Tumor sizes were measured weekly using calipers and volumes calculated using the standard formula: $\text{width}^2 \times \text{length} \times 0.52$. Tumor growth times were assessed by Kaplan-Meier analysis [37], with survival defined as the period from the onset of treatment to a tumor size of 2000 mm^3 (the point of animal sacrifice, in accordance with our animal use protocol). Log-rank tests were used for statistical comparisons.

Results

OSU-HDAC42 Exhibits Antigrowth Activity against Ovarian Cancer, But Not Normal, Epithelial Cells

To examine the antiproliferative activity of OSU-HDAC42 against ovarian cancer, three cell lines were used: 1) A2780 (cisplatin-sensitive); 2) CP70, a platinum-resistant A2780 subline generated by cisplatin selection (i.e., having "acquired resistance") [38]; and 3) OVCAR10, a cisplatin-resistant line that originated from a relapsed ovarian cancer patient (i.e., "intrinsically resistant") [39]. In comparable agreement with previous studies (which used 72-hour rather than 48-hour cisplatin exposure) [38,40], A2780 cells demonstrated a high sensitivity to cisplatin (IC_{50} value of 3.2 μM), after 48 hours of treatment, whereas CP70 and OVCAR10 were 13- to 17-fold

more resistant, with IC_{50} values of 42.6 and 53.1 μM, respectively (Figure W1). Consequently, these three cell lines could be suggested to mimic early-stage responsive (A2780 cells), never-responsive (OVCAR10 cells), and relapsed (CP70 cells) ovarian cancer patients [38,39]. However, despite these differing platinum responses, all three cell lines demonstrated low-dose sensitivities to a 48-hour OSU-HDAC42 treatment, with IC_{50} values of 0.6 μM for A2780 cells, 1.1 μM for CP70 cells, and 1.1 μM for OVCAR10 cells (Figure 1*A*),

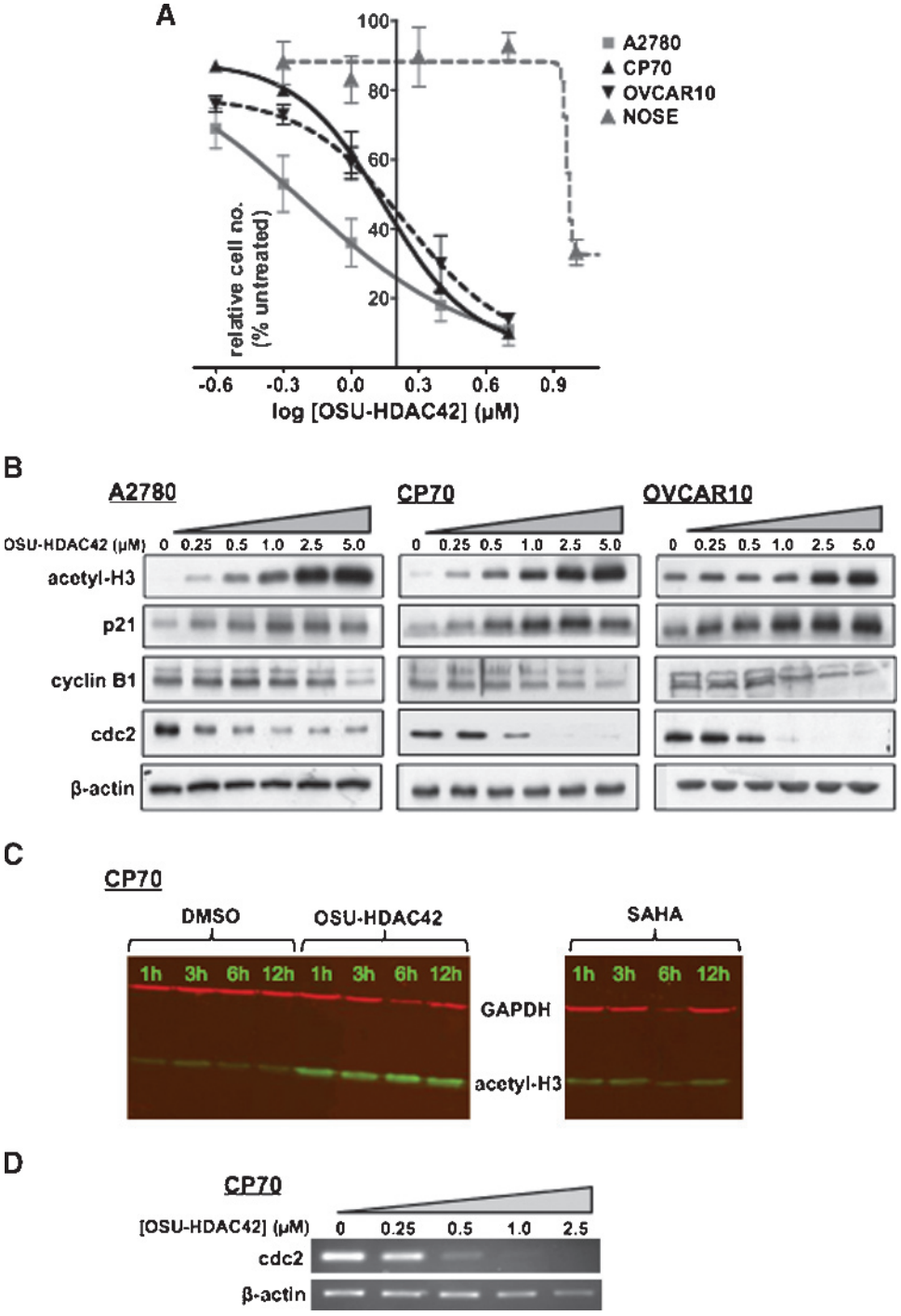

Figure 1. OSU-HDAC42–mediated growth inhibition, histone acetylation, cell cycle protein regulation, and cell cycle arrest in ovarian cancer and normal epithelial cell lines. (A) OSU-HDAC42 dose-responsive growth inhibition in cisplatin-sensitive A2780 ($p53^{+/+}$; gray boxes) and cisplatin-resistant CP70 (p53-dysfunctional; black triangles) and OVCAR10 ($p53^{+/+}$; inverted triangles) ovarian cancer cell lines (48-hour treatments) compared with NOSE (gray triangles) primary cells (5-day treatments). Means ± SE. (B) Forty-eight–hour dose-dependent OSU-HDAC42–induced acetylation of histone H3 and regulation of cell cycle–inhibitory (p21) and cell cycle–progression (cyclin B1 and cdc2) proteins (loading control, β-actin). (C) A direct comparison of CP70 cell histone H3 acetylation after OSU-HDAC42 *versus* SAHA treatment (both at 1.0 μM for 1-12 hours). (D) Reverse transcription–PCR analysis of OSU-HDAC42 transcriptional regulation of the cyclin-dependent kinase-encoding gene *cdc2* in CP70 cells.

indicating potent cytoxicity of this compound regardless of cisplatin-resistant phenotype. In a similar, direct comparison, growth-inhibition studies (72-hour treatments) of three ovarian cancer cell lines, OSU-HDAC42 IC_{50} doses were found to be comparable to or less than those for SAHA (Table W2).

As a control for toxicity, we examined the effects of OSU-HDAC42 on primary NOSE cells [31]. Owing to the slower growth of NOSE cells [30,31], drug treatments were extended to 5 days to allow for a similar number of cell divisions. As shown in Figure 1*A*, OSU-HDAC42 was more than eight-fold less toxic to NOSE cells (IC_{50} of 8.9 μM) than to A2780, CP70, or OVCAR10 cells, demonstrating this agent to be antiproliferative to ovarian tumor cells at doses nontoxic to the normal epithelium from which they derive.

OSU-HDAC42 Induces G_2/M Cell Cycle Arrest by Uniquely Altering Expression of the Cell Cycle Regulators p21, cdc2, and cyclin B1

As the characteristic effects of known HDACIs include acetylation of both histone and nonhistone proteins, up- or down-regulation of specific gene products, and cell cycle arrest [10], we examined OSU-HDAC42 for these (or its own unique) mechanistic activities. Analogous to previously characterized HDACIs [5,6], the 48-hour treatment with OSU-HDAC42 substantially enhanced acetylation of bulk histone H3 in all three cell lines (Figure 1*B*); additionally, acetylation was more pronounced, at 1 μM, than the identical treatment with SAHA (Figure 1*C*). In addition, the expression of the cell cycle inhibitor p21 was elevated by OSU-HDAC42, whereas the G_2/M cell cycle progression proteins cdc2 and cyclin B1 were downregulated (Figure 1*B*) [41]; moreover, semiquantitative reverse transcription–PCR revealed cdc2 down-regulation to occur at the messenger RNA (mRNA) level (Figure 1*D*).

As dysregulation of cell cycle regulatory proteins suggests an altered cell cycle distribution, we performed flow cytometry to quantitate DNA content after OSU-HDAC42 treatment by PI DNA staining. As shown in Table 1, G_2/M fractions of A2780 and CP70 were substantially (more than five-fold) elevated in a dose-dependent manner, with only a two-fold increase in the OVCAR10 G_2/M index. In CP70 and A2780 cells, the G_1 fraction demonstrated a slight but definite decrease at the higher (2.5 and 5.0 μM) doses, whereas no G_1 change was observed in OVCAR10 cells. Thus, in accord with the protein expression results (Figure 1*B*), OSU-HDAC42–mediated G_2/M cell cycle arrest roughly correlated with p21 up-regulation and down-regulation of both cdc2 and cyclin B1.

To further examine the transcriptional regulation of cell cycle proteins and a possible role for the p53 tumor suppressor in OSU-HDAC42–treated ovarian cancer cells, we performed quantitative reverse transcription–PCR analysis of the p53-dependent, proapoptotic gene *NOXA* [42], the partially p53-regulated gene *p21* (*p21* is also directly induced by histone hyperacetylation) [6], and two p53-independent genes, *Apaf-1* and *γ-globin*, in A2780 (p53-positive) and CP70 (p53-null) cells treated with 1 μM drug for 24 hours. As shown in Figure W2, both OSU-HDAC42 and SAHA induced *NOXA* in A2780 cells (*A*) but not in CP70 cells (*B*). Similarly, OSU-HDAC42 induced *p21* by 7- and 4.5-fold in A2780 and CP70 cells, respectively, with corresponding SAHA-induced increases of 5.3- and 2.4-fold. Whereas that result differed somewhat from the p21 Western blot (Figure 1*B*), it is difficult to presume that protein levels (based on stability for 48 hours) would mimic mRNA induction (during a 24-hour period). In contrast, the two p53-independent genes, *Apaf-1* and *γ-globin*, were not differentially upregulated by either HDACI in A2780 *versus* CP70 cells. These findings, in addition to the higher IC_{50} for OSU-HDAC42 in CP70 cells (Figure 1*A*), suggest that OSU-HDAC42, at least in part, interacts with the p53 tumor suppressor pathway.

Table 1. Dose-Dependent Effects of OSU-HDAC42 on Cell Cycle Distributions in A2780, CP70, and OVCAR10 Cells.

[OSU-HDAC42] (μM)		0	0.25	0.5	1.0	2.5	5.0
A2780	G_1 (%)	49	56	58	56	46	43
	S (%)	41	29	19	13	8	8
	G_2/M (%)	9	15	22	31	46	49
CP70	G_1 (%)	55	47	53	60	41	31
	S (%)	35	39	30	13	10	12
	G_2/M (%)	10	14	17	27	50	56
OVCAR10	G_1 (%)	60	63	69	72	67	68
	S (%)	28	24	20	4	5	4
	G_2/M (%)	12	13	11	24	29	28

Dose-Dependent Acetylation of α-Tubulin and Induction of Apoptosis by OSU-HDAC42

As mentioned in a previous paragraph, it is now well established that numerous nonhistone proteins are also HDAC substrates [6,43]. Because α-tubulin is often hyperacetylated after HDACI treatment [44], we examined the acetylation status of this microtubule-associated protein in HDACI-treated cells. As shown in Figure 2*A*, α-tubulin was highly acetylated, even at low (0.25 μM) OSU-HDAC42 doses, in both A2780 (*left panel*) and CP70 (*right panel*) cells. Moreover, in CP70 cells, α-tubulin acetylation was more pronounced after 1 μM OSU-HDAC42 treatment than with 1 μM SAHA (Figure 2*B*). Because those two agents possess fairly similar structures (according to Lipinsky's rules of drug-like properties) [45], their cellular uptake (i.e., membrane permeability) would likely be comparable. Consequently, these tubulin deacetylase inhibition results might suggest a greater biochemical potency for OSU-HDAC42 compared with SAHA.

Because α-tubulin acetylation by HDACIs has previously been associated with apoptosis [44], we investigated the effects of OSU-HDAC42 on cell death by three independent assessments: 1) PI stain–based sub-G_1 cell fraction analysis (i.e., detection of cells with fragmented DNA), 2) apoptotic cleavage of the DNA repair enzyme poly(ADP) ribosylase polymerase (PARP), and 3) annexin V–FITC staining of externalized plasma membrane phosphatidylserine, in conjunction with PI DNA staining of nonviable cells. As shown in Figure 3*A*, OSU-HDAC42 dose-dependently (0-2.5 μM) induced sub-G_1 cell accumulation in all three cell lines tested. Similarly, PARP cleavage (Figure 3*B*) and annexin V/PI staining (Figure 3*C*) demonstrated similar OSU-HDAC42 dose dependencies. Thus, in agreement with the results of our cell cycle analyses (Table 1), the CP70 and A2780 ovarian cancer cell lines showed relatively low-dose (approximately 1 μM) susceptibilities to OSU-HDAC42–induced apoptosis, whereas OVCAR10 cells required a greater dose (2.5 μM) for substantial apoptosis.

OSU-HDAC42–Induced Cell Morphology Changes and Epithelial Differentiation

To evaluate possible effects of OSU-HDAC42 on cancer cell differentiation, as reported for other HDACIs [46,47], we examined

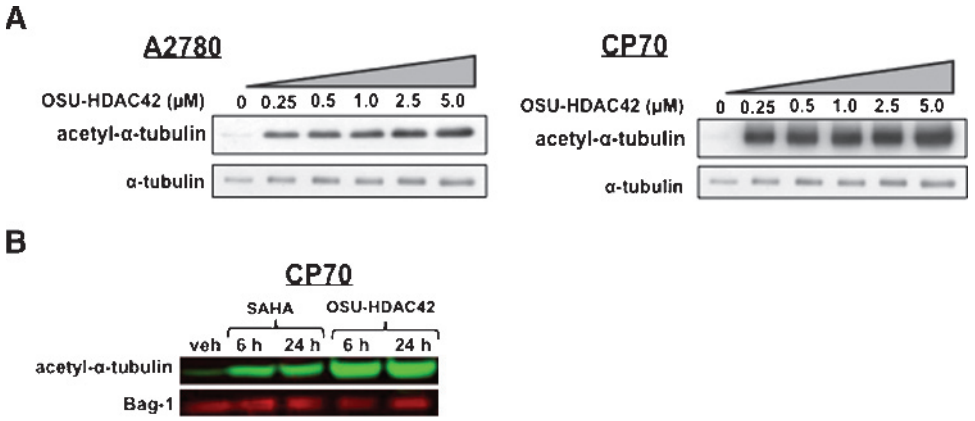

Figure 2. OSU-HDAC42–induced acetylation of histone H3 and α-tubulin, in comparison to the HDAC inhibitor SAHA. (A) OSU-HDAC42 dose-dependent α-tubulin acetylation in A2780 (left panel) and CP70 (right panel) cells. (B) A direct comparison of SAHA- *versus* OSU-HDAC42–mediated tubulin acetylation after 1 μM drug treatment for 6 or 24 hours.

changes in ovarian cancer cell morphology and cytokeratin expression after OSU-HDAC42 treatment. As shown in Figure 4*A*, the 24-hour OSU-HDAC42 treatment resulted in dose-dependent, progressive morphological changes from round to flat/elongated in both cisplatin-sensitive (A2780; *upper panel*) and -resistant (CP70; *lower panel*) cells. These changes in cell morphology were also associated with increases in cytokeratin expression as determined by immunocytochemistry. As shown in Figure 4*B*, the 48-hour OSU-HDAC42 treatment of A2780 and CP70 cells resulted in diaminobenzidine staining (brown stain) of the pan-cytokeratin monoclonal antibody cocktail AE1/AE3 [34], demonstrating up-regulation of these epithelium-specific markers. To quantitate cytokeratin expression, flow cytometric assessment revealed dose-dependent increases in AE1/AE3 binding (Figure 4*B*, *inset numbers*) in both cell lines after the 48-hour OSU-HDAC42 treatment. Together, these results support the induction of epithelial differentiation in ovarian cancer cells after treatment with OSU-HDAC42.

OSU-HDAC42 Sensitizes Platinum-Resistant CP70 Cells to Cisplatin-Induced Apoptosis

In a previous study, OSU-HDAC42 was demonstrated to resensitize chemoresistant DU-145 prostate cancer cells to various agents that induce double-strand DNA breakage by acetylation of the DNA repair enzyme Ku70 [23]. Although the role of Ku70 in response to platinum drugs (routinely used against advanced ovarian cancer and which induce the formation of bulky DNA adducts rather than double strand breaks) [48] is fairly controversial [24,25], we examined whether OSU-HDAC42 could similarly elicit chemosensitization to these commonly used chemotherapeutics. Additional rationale for the assessment of OSU-HDAC42 cisplatin sensitization was based on the evidence of OSU-HDAC42–induced epithelial differentiation in the cisplatin-resistant cell line CP70 (described previously mentioned) and recent hypotheses implicating poorly differentiated tumor progenitors in drug resistance [49]. CP70 cells were pretreated with OSU-HDAC42 for 4 hours at 1.0 μM (the IC_{50} value for CP70; Figure 1*A*) followed by treatment with increasing concentrations of cisplatin for 2 days and assessment of cell viability by MTT assay. As shown in Figure 5*A*, HDACI pretreatment substantially increased the sensitivity of CP70 cells to cisplatin, lowering its IC_{50} value more than 30-fold (analysis not shown). Similar drug response analyses (Figure W3) revealed no OSU-HDAC42 enhancement of cisplatin's effects on the already-sensitive A2780 cells (*A*), whereas highly chemoresistant OVCAR10 cells demonstrated increased cisplatin sensitivity, similar to that observed in CP70 cells, after 1.0 μM (the OVCAR10 IC_{50} dose) HDACI pretreatment (*B*). To assess whether this loss of CP70 cell number (as shown by MTT assays), after the combination treatment, was due to apoptosis, cisplatin-induced PARP cleavage was examined with or without OSU-HDAC42 pretreatment. As shown in Figure 5*B*, the OSU-HDAC42/cisplatin combination caused a marked enhancement of PARP cleavage at 25 μM cisplatin indicating induction of apoptosis. Similar to the PARP analysis, a second assessment of apoptosis in CP70 cells using annexin V/FITC flow cytometric analysis (Figure 5*C*) indicated that whereas OSU-HDAC42 alone induced apoptosis (23% FITC-positive cells), an enhanced effect (in combination with 1.0 μM OSU-HDAC42) was observed at 25 μM cisplatin (38% annexin-labeled cells) compared with cisplatin alone (5% annexin-labeled cells). Analysis of those OSU-HDAC42/cisplatin combinations revealed an additive but not synergistic effect of the HDAC inhibitor on cisplatin sensitivity (analysis not shown).

Also in agreement with MTT assays, OSU-HDAC42 pretreatment of chemosensitive A2780 cells resulted in no apparent increase in PARP cleavage in cisplatin-treated cells (Figures W3 and W4*A*). However, the annexin V/FITC analyses of that cell line was somewhat contradictory to the other two cell viability assessments, with A2780 showing additive OSU-HDAC42/cisplatin effects (Figure W4*B*). On the basis of the presence of both PI and annexin V staining (*upper right quadrants*; double-positive cells), it is possible that these cells underwent necrosis as well as apoptosis [50].

In Vivo *Antitumor Platinum Sensitization of Cisplatin-Resistant CP70 Xenograft Tumors*

On the basis of its chemosensitizing and differentiating effects (Figures 4 and 5), we evaluated the effects of OSU-HDAC42 on the growth of CP70 xenograft tumors, alone or in combination with cisplatin, in immunodeficient (NCr-*nu*/*nu*) nude mice. After subcutaneous injection of 5×10^5 CP70 cells, mice bearing established tumors (100 mm^3) were randomized to eight distinct treatment groups (see Materials and Methods and Table W1), with doses based

on similar HDACI and cisplatin mouse xenograft studies [35,36]. Tumor growth was assessed by Kaplan-Meier analysis [37], with survival duration defined as the time for tumors to reach a volume of 2000 mm^3. As shown in Figure 6*A*, the combination treatment of OSU-HDAC42, at 50 mg/kg, with cisplatin (purple line) significantly prolonged survival, that is, delayed tumor growth (P = .0021, log-rank test) compared with vehicle control (*blue line*). In contrast, daily treatment with SAHA, both singly, at 50 and 25 mg/kg (data not shown), and in combination with cisplatin, did not significantly inhibit tumor growth in this model (Figure 6*B*). These data suggest that OSU-HDAC42 can resensitize platinum-resistant ovarian tumors to cisplatin *in vivo*.

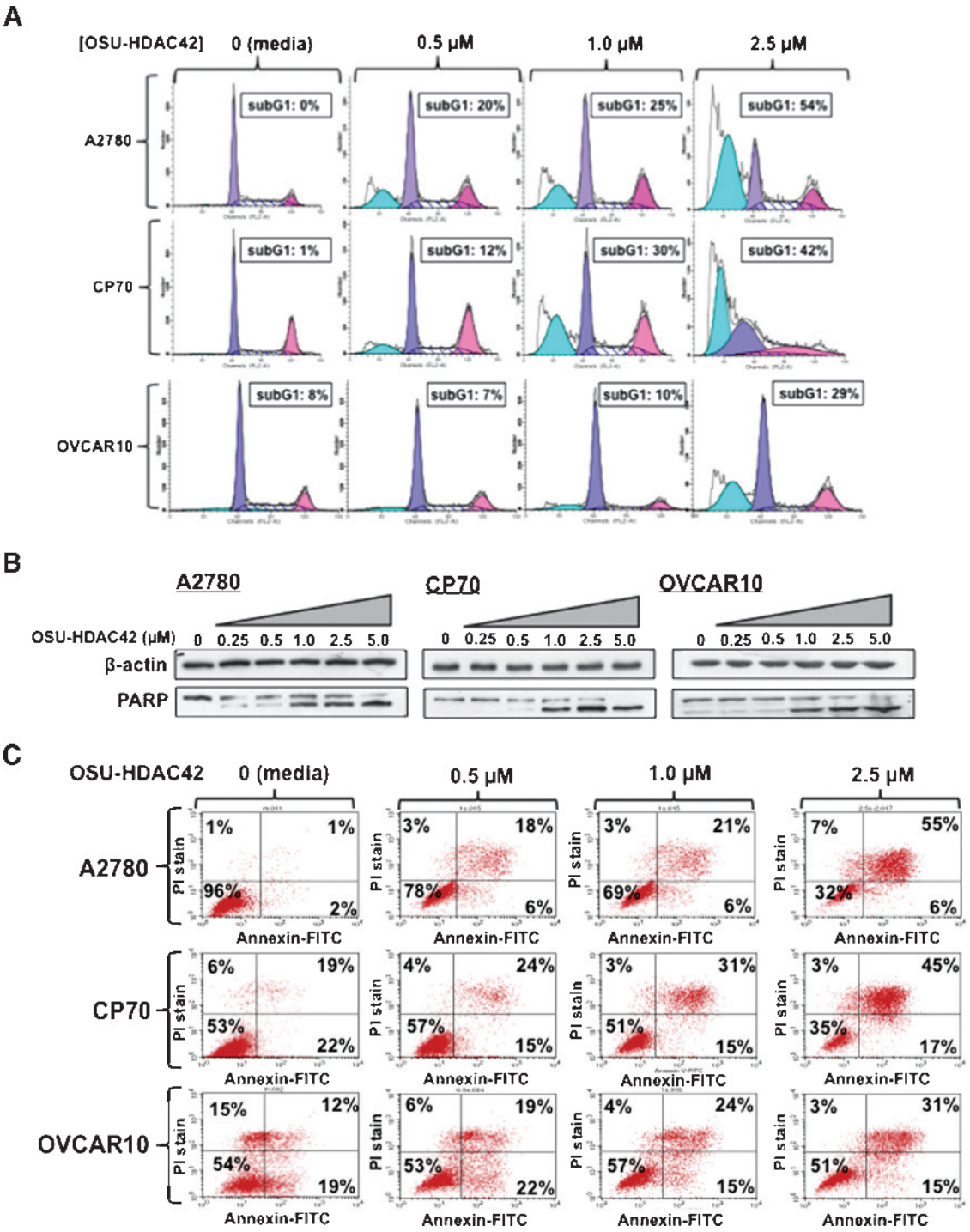

Figure 3. Further examination of apoptotic events induced dose-dependently by a 48-hour OSU-HDAC42 treatment of A2780, CP70, and OVCAR10 cells, including (A) a 48-hour OSU-HDAC42 dose-dependent accumulation of sub-G_1 (i.e., sub-2N) DNA (representing apoptotic cellular debris) after treatment of A2780, CP70, and OVCAR10 cells, as assessed by flow cytometric analysis of PI-stained, fixed, and permabilized cells. (B) Poly(ADP-ribose) polymerase cleavage by caspase 3. (C) Annexin V–FITC binding to membrane-exposed phosphatidylserine concomitant with PI viability staining.

Discussion

Intracellular protein acetylation is intimately involved in numerous biological processes, including cell growth, intracellular signaling, and gene regulation [43], and a disrupted "acetylome" (i.e., the total acetylation state of a cell) is well associated with neoplasia [6]. Histone deacetylase inhibitors (HDACIs) are a family of compounds originally discovered as inducers of erythroleukemia cell differentiation [3]; these differentiating agents were only later discovered to increase histone acetylation through the inhibition of deacetylase enzymes [4]. In preclinical studies of ovarian cancer, a number of HDACIs have demonstrated impressive antiproliferative (and generally nontoxic) effects against cultured cells and xenograft tumors. In one study, the long-standing anticonvulsant, VPA (Depakote), impressively (~80%) suppressed the growth of xenograft tumors of the ovarian cancer cell line SKOV3, with significant p21 up-regulation in tumor tissues [51]. Despite encouraging preclinical studies, however, VPA has proved fairly disappointing in clinical trials for myeloid malignancies [52], diminishing optimism for its eventual use against human solid tumors. Another rationally designed hydroxamic acid HDACI, PXD-101 (belinostat), has demonstrated impressive antitumor effects against aggressive ovarian cancer xenografts [53,54] and is now in clinical trials. Overall, however, in contrast to hematologic malignancies, single-agent trials of HDACIs for solid tumors, including ovarian cancer, have only rarely demonstrated measurable patient responses [8,9,11].

Whereas HDACIs may lack efficacy as monotherapies, it is generally agreed that these agents will be most effective in combination with other agents [5,9]. In a preclinical study similar to our current work, VPA was found to resensitize CP70 and other resistant ovarian cancer cell lines to cisplatin, although the cisplatin IC_{50} values reported in that study (A2780, 0.25 μM; CP70, 5.0 μM, using a shorter 24-hour treatment) [55] were much lower than those we observed (A2780, 3.2 μM; CP70, 42.6 μM, 48-hour treatment; Figure W1). Consequently, because single-agent cisplatin was found to be much more cytotoxic than in our study, the actual resensitization by VPA pretreatment (in that work) was greatly diminished compared with the OSU-HDAC42–mediated resensitization that we report here (Figure 5). In other preclinical studies, the benzamide HDACI M344 was found to inhibit the growth of SKOV3 ovarian cancer cells with an IC_{50} of 5.1 μM [56], a lower potency than OSU-HDAC42 against similarly aggressive malignant cell lines (Figure 1*A*). Another hydroxamate HDACI, trichostatin A (TSA), was found to activate the oncogenic EGFR/Akt signaling pathway in CAOV3 ovarian cancer cells [57], a finding that is in direct contrast to OSU-HDAC42, which induces the dephosphorylation and inactivation of Akt [22]. In another study, however, TSA was found to enhance the sensitivity of ovarian cancer cells to various DNA-damaging agents [58], an activity also attributed to OSU-HDAC42, which sensitizes prostate cancer cells to agents that induce DNA double-strand breaks through the hyperacetylation (and subsequent suppression of DNA-binding activity) of the DNA repair protein Ku70 [23].

Mechanistically, it seems that the effects of OSU-HDAC42 are distinct from most previously studied hydroxamic acid HDACIs. Whereas most HDACIs exert G_1 arrest [5,29] or abrogate a G_2 checkpoint [59], OSU-HDAC42 was found to cause G_2-phase cell accumulation and, interestingly, a distinct G_1 fraction decrease in cisplatin-resistant CP70 cells (Table 1). Moreover, this G_2 arrest may occur through an unconventional mechanism. Whereas OSU-HDAC42

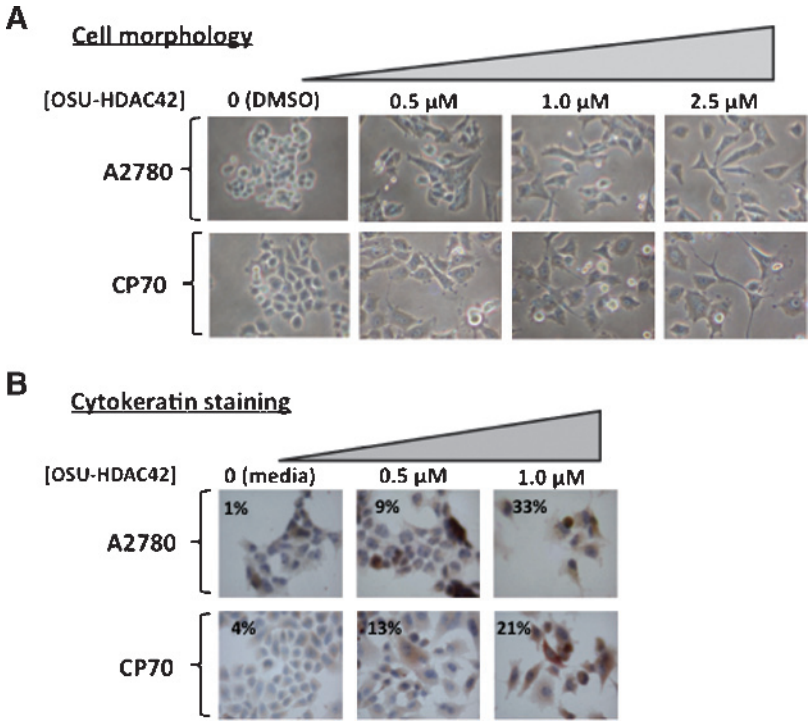

Figure 4. OSU-HDAC42–induced epithelial differentiation of ovarian cancer cells. (A) Dose-dependent morphologic changes after a 24-hour OSU-HDAC42 treatment of A2780 (upper panel) and CP70 (lower panel) cells. (B) Up-regulation of numerous cytokeratins (as assessed by AE1/AE3 monoclonal antibody cocktail staining) in A2780 (upper panel) and CP70 (lower panel) cells after a 48-hour OSU-HDAC42 treatment. Inset numbers: flow cytometric quantification of AE1/AE3–positive CP70 cells.

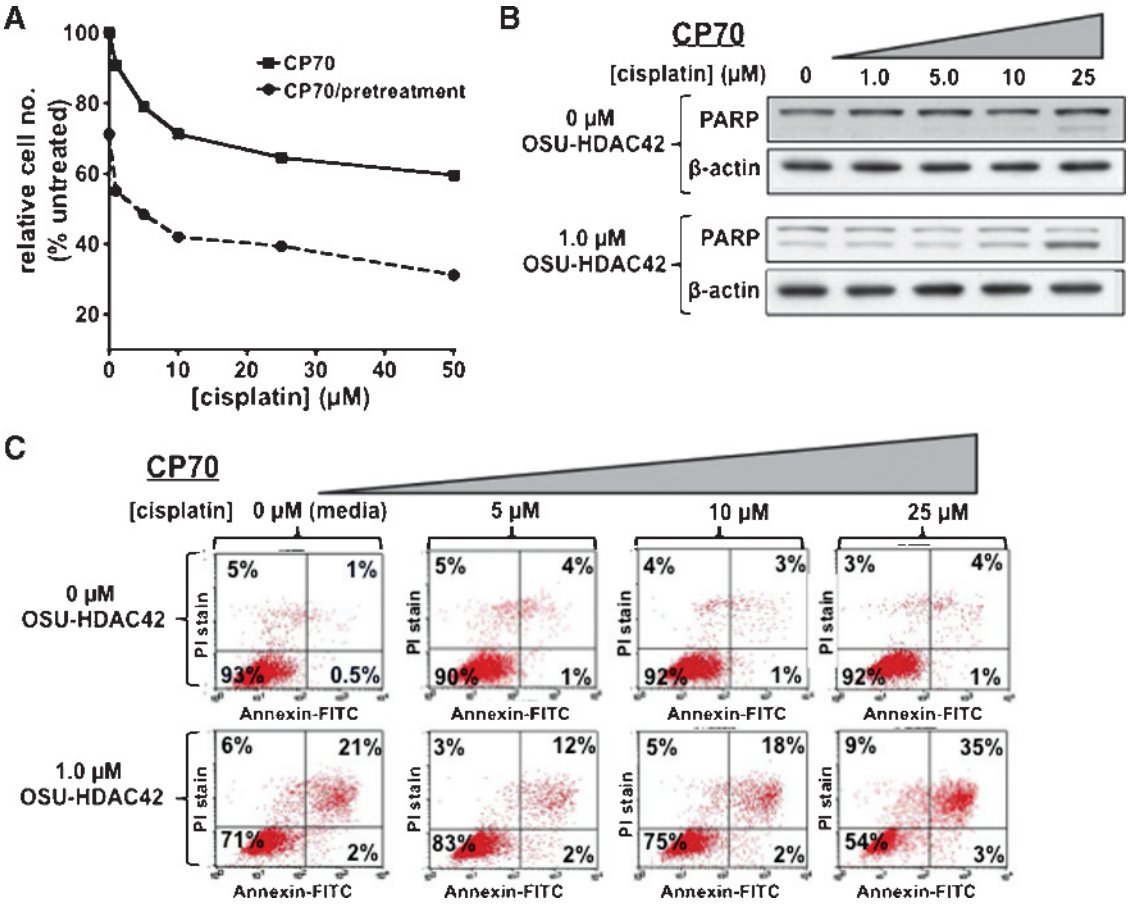

Figure 5. OSU-HDAC42–mediated chemosensitization and apoptosis of platinum-resistant CP70 ovarian cancer cells to cisplatin. Cells were pretreated for 4 hours with 1.0 μM OSU-HDAC42 (CP70 IC_{50} dose) followed by a 48-hour treatment with media or 1, 5, 10, 25, or 50 μM cisplatin. Cisplatin sensitivities were then assessed by (A) MTT cell viability assay, (B) PARP cleavage by caspase 3, and (C) annexin V fluorescent staining of externalized phosphatidylserine (an early apoptotic event) coupled with PI staining for loss of membrane integrity.

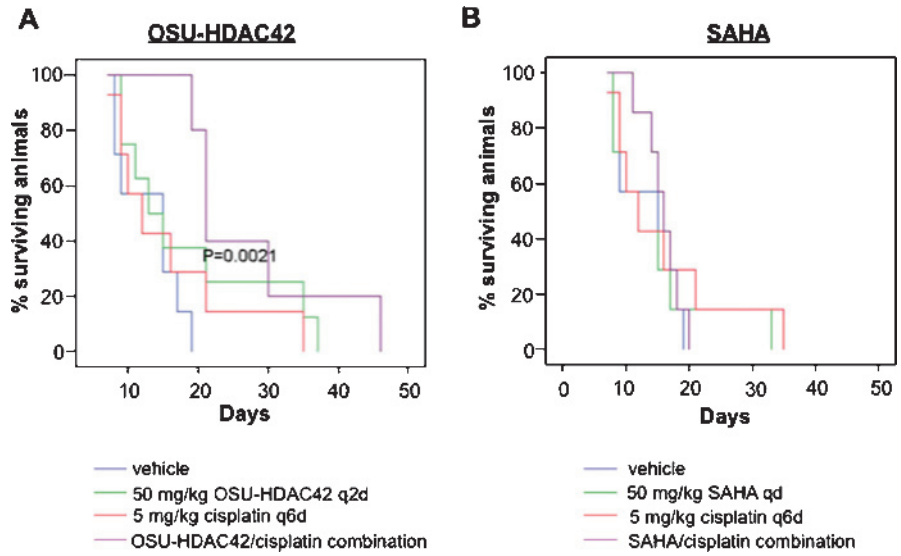

Figure 6. Kaplan-Meier survival analysis of CP70 tumor-bearing athymic nude mice treated with OSU-HDAC42 (A) or SAHA (B) alone or in combination with cisplatin. Survival was based on the length of time after CP70 cell subcutaneous engraftment for a specific animal's tumor to reach a volume of 2000 mm^3 (time of animal sacrifice). See Materials and Methods and Table W1 for a description of mouse treatment groups (eight randomized mice per group). As shown, only the OSU-HDAC42/cisplatin combination treatment group demonstrated prolonged survival (P = .0021).

elicited down-regulation of cyclin B1 (Figure 1*B*), an event previously associated with other HDACIs [5,60], we also observed a likely transcriptional repression (although we cannot rule out mRNA degradation) of the cyclin-dependent kinase-encoding gene *cdc2*, which, to our knowledge, is a previously unreported HDACI-associated phenomenon. Although the mechanism of *cdc2* transcriptional repression remains uncertain, it has been reported that HDACIs can restore p53 function to cells harboring mutations in that specific tumor suppressor [61] and also that p53 interference with NF-Y–mediated transactivation can downregulate *cdc2* [62]. Moreover, the p53 transcription factor itself is acetylated (and thus activated) through HDACI inhibition of HDAC6 [5,9]. Another possible mechanism for *cdc2* silencing could be through OSU-HDAC42 up-regulation of the expression and/or activity of the cell cycle–dependent element–binding factor 1, a repressor of *cdc2* and other growth-promoting genes [63]. Interestingly, HDACIs have also been demonstrated to downregulate specific genes (including cyclin B1) [60] by histone *deacetylation*, possibly due to the induction of NADH-dependent class III HDACs, which are not inhibited by zinc-chelating hydroxamic acid HDACIs [64].

Although not a clinically viable HDACI [5], contrasting the effects of TSA with those of OSU-HDAC42 may prove informative regarding the antitumor mechanism(s) of the latter compound. As shown in Table 1, OSU-HDAC42 was found to induce prominent G_2 arrest in both cisplatin-resistant (CP70) and -sensitive (A2780) cells, with a lesser G_2 effect noted in OVCAR10 cells. A smaller-magnitude G_1 arrest was also observed in the former two cell lines; however, the G_1 fraction was relatively unchanged in OVCAR10 cells, which also possessed a much lower S-phase index, in agreement with a previous report comparing the relative radiosensitivity of these various ovarian cancer cells [65]. Trichostatin A, by contrast, was previously found to shift its mode of cell cycle arrest from G_1 to G_2 upon the acquisition of cisplatin resistance (i.e., elicit G_1 blockage in A2780 cells, with G_2 accumulation of CP70 cells) [47]. Also, in contrast to OSU-HDAC42, TSA was demonstrated to bypass mitochondrial apoptosis in CP70 cells, through the up-regulation of p73 and Bax [66]. Although we did not examine intrinsic *versus* extrinsic apoptosis in this work, other studies demonstrating that OSU-HDAC42 elicits cytochrome *C* cytosolic accumulation [19] and down-regulation of Bcl-xL [21], suggest (at least partial) induction of cell death by mitochondria-associated cascades. Thus, OSU-HDAC42 exerts its antineoplastic activity much differently than TSA, despite the two agents having similar zinc-chelating (hydroxamate) moieties.

One topic of current debate is whether isoform-specific or pan-HDAC inhibitors will be most effective as antitumor agents [9,10]. Although no assessments of the effect of OSU-HDAC42 on specific HDAC isoforms have been performed, based on studies to date [19,21–23], it is fairly certain that OSU-HDAC42 is a pan-HDAC inhibitor as demonstrated by its inhibition of both class I (histone-deacetylating) and class II (including HDAC6, the deacetylase of tubulin) [67] enzymes. Whereas the issue of the clinical superiority of pan- *versus* isoform-specific HDAC inhibitors remains an open question, acetylation of tubulin, previously correlated with HDACI-induced apoptosis [44], may be indispensable to the antitumor activity of OSU-HDAC42. Moreover, it has recently been demonstrated that HDAC6 is essential for apoptosis resistance and tumor growth of SKOV3 ovarian cancer xenografts [68], thus supporting inhibition of that particular class II deacetylase (HDAC6), as well as class I enzymes, as necessary prerequisites for the therapy for ovarian cancer.

In summary, we demonstrate that the novel HDAC inhibitor OSU-HDAC42 is highly growth-suppressive of ovarian cancer cells and tumors and acts (at least in part) through unconventional mechanisms, with similar or greater potency than previously established hydroxamate HDACIs. Consistent with a previous mechanistic study [23], we found that OSU-HDAC42/cisplatin combinations effectively resensitize cisplatin-resistant malignant cells and delay cisplatin-resistant tumor growth in xenograft tumors *in vivo*. Overall, these results strongly indicate OSU-HDAC42 to be a promising candidate for the treatment of drug-resistant ovarian cancer, a disease in dire need of improved interventional approaches.

Acknowledgments

The authors thank Ceazon Edwards, Kaleb Nageli, and Teresa Craft for technical assistance.

References

[1] National Cancer Institute. *Ovarian Cancer (Invasive) Survival Rates, By Race, Diagnosis year, Stage and Age. SEER Cancer Statistics Review 1975-2005*. National Cancer Institute, Bethesda, MD. Available at: http://seer.cancer.gov/csr/1975_2005/.

[2] Ozols RF (2005). Treatment goals in ovarian cancer. *Int J Gynecol Cancer* **15** (Suppl 1), 3–11.

[3] Orkin SH, Harosi FI, and Leder P (1975). Differentiation in erythroleukemic cells and their somatic hybrids. *Proc Natl Acad Sci USA* **72**, 98–102.

[4] Richon VM, Emiliani S, Verdin E, Webb Y, Breslow R, Rifkind RA, and Marks PA (1998). A class of hybrid polar inducers of transformed cell differentiation inhibits histone deacetylases. *Proc Natl Acad Sci USA* **95**, 3003–3007.

[5] Bolden JE, Peart MJ, and Johnstone RW (2006). Anticancer activities of histone deacetylase inhibitors. *Nat Rev Drug Discov* **5**, 769–784.

[6] Minucci S and Pelicci PG (2006). Histone deacetylase inhibitors and the promise of epigenetic (and more) treatments for cancer. *Nat Rev Cancer* **6**, 38–51.

[7] Marks PA and Breslow R (2007). Dimethyl sulfoxide to vorinostat: development of this histone deacetylase inhibitor as an anticancer drug. *Nat Biotechnol* **25**, 84–90.

[8] Garber K (2007). HDAC inhibitors overcome first hurdle. *Nat Biotechnol* **25**, 17–19.

[9] Lee MJ, Kim YS, Kummar S, Giaccone G, and Trepel JB (2008). Histone deacetylase inhibitors in cancer therapy. *Curr Opin Oncol* **20**, 639–649.

[10] Marsoni S, Damia G, and Camboni G (2008). A work in progress: the clinical development of histone deacetylase inhibitors. *Epigenetics* **3**, 164–171.

[11] Modesitt SC, Sill M, Hoffman JS, and Bender DP (2008). A phase II study of vorinostat in the treatment of persistent or recurrent epithelial ovarian or primary peritoneal carcinoma: a Gynecologic Oncology Group study. *Gynecol Oncol* **109**, 182–186.

[12] Wang DF, Helquist P, Wiech NL, and Wiest O (2005). Toward selective histone deacetylase inhibitor design: homology modeling, docking studies, and molecular dynamics simulations of human class I histone deacetylases. *J Med Chem* **48**, 6936–6947.

[13] Finnin MS, Donigian JR, Cohen A, Richon VM, Rifkind RA, Marks PA, Breslow R, and Pavletich NP (1999). Structures of a histone deacetylase homologue bound to the TSA and SAHA inhibitors. *Nature* **401**, 188–193.

[14] Richon VM, Webb Y, Merger R, Sheppard T, Jursic B, Ngo L, Civoli F, Breslow R, Rifkind RA, and Marks PA (1996). Second generation hybrid polar compounds are potent inducers of transformed cell differentiation. *Proc Natl Acad Sci USA* **93**, 5705–5708.

[15] Jung M, Brosch G, Kolle D, Scherf H, Gerhauser C, and Loidl P (1999). Amide analogues of trichostatin A as inhibitors of histone deacetylase and inducers of terminal cell differentiation. *J Med Chem* **42**, 4669–4679.

[16] Marks PA (2007). Discovery and development of SAHA as an anticancer agent. *Oncogene* **26**, 1351–1356.

[17] Ueda H, Manda T, Matsumoto S, Mukumoto S, Nishigaki F, Kawamura I, and Shimomura K (1994). FR901228, a novel antitumor bicyclic depsipeptide produced by *Chromobacterium violaceum* No. 968. III. Antitumor activities on experimental tumors in mice. *J Antibiot (Tokyo)* **47**, 315–323.

[18] Lu Q, Wang DS, Chen CS, Hu YD, and Chen CS (2005). Structure-based optimization of phenylbutyrate-derived histone deacetylase inhibitors. *J Med Chem* **48**, 5530–5535.

[19] Kulp SK, Chen CS, Wang DS, Chen CY, and Chen CS (2006). Antitumor effects of a novel phenylbutyrate-based histone deacetylase inhibitor, (*S*)-HDAC-42, in prostate cancer. *Clin Cancer Res* **12**, 5199–5206.

[20] Sargeant AM, Rengel RC, Kulp SK, Klein RD, Clinton SK, Wang YC, and Chen CS (2008). OSU-HDAC42, a histone deacetylase inhibitor, blocks prostate tumor progression in the transgenic adenocarcinoma of the mouse prostate model. *Cancer Res* **68**, 3999–4009.

[21] Lu YS, Kashida Y, Kulp SK, Wang YC, Wang D, Hung JH, Tang M, Lin ZZ, Chen TJ, Cheng AL, et al. (2007). Efficacy of a novel histone deacetylase inhibitor in murine models of hepatocellular carcinoma. *Hepatology* **46**, 1119–1130.

[22] Chen CS, Weng SC, Tseng PH, and Lin HP (2005). Histone acetylation–independent effect of histone deacetylase inhibitors on Akt through the reshuffling of protein phosphatase 1 complexes. *J Biol Chem* **280**, 38879–38887.

[23] Chen CS, Wang YC, Yang HC, Huang PH, Kulp SK, Yang CC, Lu YS, Matsuyama S, Chen CY, and Chen CS (2007). Histone deacetylase inhibitors sensitize prostate cancer cells to agents that produce DNA double-strand breaks by targeting Ku70 acetylation. *Cancer Res* **67**, 5318–5327.

[24] Townsend DM, Shen H, Staros AL, Gate L, and Tew KD (2002). Efficacy of a glutathione *S*-transferase pi–activated prodrug in platinum-resistant ovarian cancer cells. *Mol Cancer Ther* **1**, 1089–1095.

[25] Shao CJ, Fu J, Shi HL, Mu YG, and Chen ZP (2008). Activities of DNA-PK and Ku86, but not Ku70, may predict sensitivity to cisplatin in human gliomas. *J Neurooncol* **89**, 27–35.

[26] Cannistra SA (2004). Cancer of the ovary. *N Engl J Med* **351**, 2519–2529.

[27] Chan MW, Huang YW, Hartman-Frey C, Kuo CT, Deatherage D, Qin H, Cheng AS, Yan PS, Davuluri RV, Huang TH, et al. (2008). Aberrant transforming growth factor beta1 signaling and SMAD4 nuclear translocation confer epigenetic repression of ADAM19 in ovarian cancer. *Neoplasia* **10**, 908–919.

[28] Weichert W, Denkert C, Noske A, Darb-Esfahani S, Dietel M, Kalloger SE, Huntsman DG, and Kobel M (2008). Expression of class I histone deacetylases indicates poor prognosis in endometrioid subtypes of ovarian and endometrial carcinomas. *Neoplasia* **10**, 1021–1027.

[29] Vanhaecke T, Papeleu P, Elaut G, and Rogiers V (2004). Trichostatin A–like hydroxamate histone deacetylase inhibitors as therapeutic agents: toxicological point of view. *Curr Med Chem* **11**, 1629–1643.

[30] Ahluwalia A, Yan P, Hurteau JA, Bigsby RM, Jung SH, Huang TH, and Nephew KP (2001). DNA methylation and ovarian cancer. I. Analysis of CpG island hypermethylation in human ovarian cancer using differential methylation hybridization. *Gynecol Oncol* **82**, 261–268.

[31] Kruk PA, Maines-Bandiera SL, and Auersperg N (1990). A simplified method to culture human ovarian surface epithelium. *Lab Invest* **63**, 132–136.

[32] Chou TC (1976). Derivation and properties of Michaelis-Menten type and Hill type equations for reference ligands. *J Theor Biol* **59**, 253–276.

[33] Livak KJ and Schmittgen TD (2001). Analysis of relative gene expression data using real-time quantitative PCR and the 2(−Delta Delta C(T)) method. *Methods* **25**, 402–408.

[34] Goddard MJ, Wilson B, and Grant JW (1991). Comparison of commercially available cytokeratin antibodies in normal and neoplastic adult epithelial and non-epithelial tissues. *J Clin Pathol* **44**, 660–663.

[35] Butler LM, Agus DB, Scher HI, Higgins B, Rose A, Cordon-Cardo C, Thaler HT, Rifkind RA, Marks PA, and Richon VM (2000). Suberoylanilide hydroxamic acid, an inhibitor of histone deacetylase, suppresses the growth of prostate cancer cells *in vitro* and *in vivo*. *Cancer Res* **60**, 5165–5170.

[36] Clarke PA, Pestell KE, Di Stefano F, Workman P, and Walton MI (2004). Characterisation of molecular events following cisplatin treatment of two curable ovarian cancer models: contrasting role for p53 induction and apoptosis *in vivo*. *Br J Cancer* **91**, 1614–1623.

[37] Buchler P, Reber HA, Lavey RS, Tomlinson J, Buchler MW, Friess H, and Hines OJ (2004). Tumor hypoxia correlates with metastatic tumor growth of pancreatic cancer in an orthotopic murine model. *J Surg Res* **120**, 295–303.

[38] Behrens BC, Hamilton TC, Masuda H, Grotzinger KR, Whang-Peng J, Louie KG, Knutsen T, McKoy WM, Young RC, and Ozols RF (1987). Characterization of a *cis*-diamminedichloroplatinum(II)–resistant human ovarian cancer cell line and its use in evaluation of platinum analogues. *Cancer Res* **47**, 414–418.

[39] Johnson SW, Laub PB, Beesley JS, Ozols RF, and Hamilton TC (1997). Increased platinum-DNA damage tolerance is associated with cisplatin resistance and cross-resistance to various chemotherapeutic agents in unrelated human ovarian cancer cell lines. *Cancer Res* **57**, 850–856.

[40] Roberts D, Schick J, Conway S, Biade S, Laub PB, Stevenson JP, Hamilton TC, O'Dwyer PJ, and Johnson SW (2005). Identification of genes associated with platinum drug sensitivity and resistance in human ovarian cancer cells. *Br J Cancer* **92**, 1149–1158.

[41] Porter LA and Donoghue DJ (2003). Cyclin B1 and CDK1: nuclear localization and upstream regulators. *Prog Cell Cycle Res* **5**, 335–347.

[42] Yu J and Zhang L (2005). The transcriptional targets of p53 in apoptosis control. *Biochem Biophys Res Commun* **331**, 851–858.

[43] Kouzarides T (2000). Acetylation: a regulatory modification to rival phosphorylation? *EMBO J* **19**, 1176–1179.

[44] Blagosklonny MV, Robey R, Sackett DL, Du L, Traganos F, Darzynkiewicz Z, Fojo T, and Bates SE (2002). Histone deacetylase inhibitors all induce p21 but differentially cause tubulin acetylation, mitotic arrest, and cytotoxicity. *Mol Cancer Ther* **1**, 937–941.

[45] Lipinski CA, Lombardo F, Dominy BW, and Feeney PJ (2001). Experimental and computational approaches to estimate solubility and permeability in drug discovery and development settings. *Adv Drug Deliv Rev* **46**, 3–26.

[46] Strait KA, Dabbas B, Hammond EH, Warnick CT, Iistrup SJ, and Ford CD (2002). Cell cycle blockade and differentiation of ovarian cancer cells by the histone deacetylase inhibitor trichostatin A are associated with changes in p21, Rb, and Id proteins. *Mol Cancer Ther* **1**, 1181–1190.

[47] Strait KA, Warnick CT, Ford CD, Dabbas B, Hammond EH, and Ilstrup SJ (2005). Histone deacetylase inhibitors induce G_2-checkpoint arrest and apoptosis in cisplatinum-resistant ovarian cancer cells associated with overexpression of the Bcl-2–related protein Bad. *Mol Cancer Ther* **4**, 603–611.

[48] Kelland L (2007). The resurgence of platinum-based cancer chemotherapy. *Nat Rev Cancer* **7**, 573–584.

[49] Dean M, Fojo T, and Bates S (2005). Tumour stem cells and drug resistance. *Nat Rev Cancer* **5**, 275–284.

[50] Vermes I, Haanen C, Steffens-Nakken H, and Reutelingsperger C (1995). A novel assay for apoptosis. Flow cytometric detection of phosphatidylserine expression on early apoptotic cells using fluorescein labelled annexin V. *J Immunol Methods* **184**, 39–51.

[51] Takai N, Kawamata N, Gui D, Said JW, Miyakawa I, and Koeffler HP (2004). Human ovarian carcinoma cells: histone deacetylase inhibitors exhibit antiproliferative activity and potently induce apoptosis. *Cancer* **101**, 2760–2770.

[52] Kuendgen A and Gattermann N (2007). Valproic acid for the treatment of myeloid malignancies. *Cancer* **110**, 943–954.

[53] Plumb JA, Finn PW, Williams RJ, Bandara MJ, Romero MR, Watkins CJ, La Thangue NB, and Brown R (2003). Pharmacodynamic response and inhibition of growth of human tumor xenografts by the novel histone deacetylase inhibitor PXD101. *Mol Cancer Ther* **2**, 721–728.

[54] Qian X, LaRochelle WJ, Ara G, Wu F, Petersen KD, Thougaard A, Sehested M, Lichenstein HS, and Jeffers M (2006). Activity of PXD101, a histone deacetylase inhibitor, in preclinical ovarian cancer studies. *Mol Cancer Ther* **5**, 2086–2095.

[55] Lin CT, Lai HC, Lee HY, Lin WH, Chang CC, Chu TY, Lin YW, Lee KD, and Yu MH (2008). Valproic acid resensitizes cisplatin-resistant ovarian cancer cells. *Cancer Sci* **99**, 1218–1226.

[56] Takai N, Ueda T, Nishida M, Nasu K, and Narahara H (2006). M344 is a novel synthesized histone deacetylase inhibitor that induces growth inhibition, cell cycle arrest, and apoptosis in human endometrial cancer and ovarian cancer cells. *Gynecol Oncol* **101**, 108–113.

[57] Zhou C, Qiu L, Sun Y, Healey S, Wanebo H, Kouttab N, Di W, Yan B, and Wan Y (2006). Inhibition of EGFR/PI3K/AKT cell survival pathway promotes TSA's effect on cell death and migration in human ovarian cancer cells. *Int J Oncol* **29**, 269–278.

[58] Ozaki K, Kishikawa F, Tanaka M, Sakamoto T, Tanimura S, and Kohno M (2008). Histone deacetylase inhibitors enhance the chemosensitivity of tumor cells with cross-resistance to a wide range of DNA-damaging drugs. *Cancer Sci* **99**, 376–384.

[59] Qiu L, Burgess A, Fairlie DP, Leonard H, Parsons PG, and Gabrielli BG (2000). Histone deacetylase inhibitors trigger a G_2 checkpoint in normal cells that is defective in tumor cells. *Mol Biol Cell* **11**, 2069–2083.

[60] Archer SY, Johnson J, Kim HJ, Ma Q, Mou H, Daesety V, Meng S, and Hodin RA (2005). The histone deacetylase inhibitor butyrate downregulates *cyclin B1* gene expression via a p21/WAF-1–dependent mechanism in human colon cancer cells. *Am J Physiol Gastrointest Liver Physiol* **289**, G696–G703.

[61] Blagosklonny MV, Trostel S, Kayastha G, Demidenko ZN, Vassilev LT, Romanova LY, Bates S, and Fojo T (2005). Depletion of mutant p53 and cytotoxicity of histone deacetylase inhibitors. *Cancer Res* **65**, 7386–7392.

[62] Yun J, Chae HD, Choy HE, Chung J, Yoo HS, Han MH, and Shin DY (1999). p53 negatively regulates cdc2 transcription via the CCAAT-binding NF-Y transcription factor. *J Biol Chem* **274**, 29677–29682.

[63] Liu N, Lucibello FC, Korner K, Wolfraim LA, Zwicker J, and Muller R (1997). CDF-1, a novel E2F-unrelated factor, interacts with cell cycle–regulated repressor elements in multiple promoters. *Nucleic Acids Res* **25**, 4915–4920.

[64] Reid G, Metivier R, Lin CY, Denger S, Ibberson D, Ivacevic T, Brand H, Benes V, Liu ET, and Gannon F (2005). Multiple mechanisms induce transcriptional silencing of a subset of genes, including oestrogen receptor alpha, in response to deacetylase inhibition by valproic acid and trichostatin A. *Oncogene* **24**, 4894–4907.

[65] Biade S, Stobbe CC, and Chapman JD (1997). The intrinsic radiosensitivity of some human tumor cells throughout their cell cycles. *Radiat Res* **147**, 416–421.

[66] Muscolini M, Cianfrocca R, Sajeva A, Mozzetti S, Ferrandina G, Costanzo A, and Tuosto L (2008). Trichostatin A up-regulates p73 and induces Bax-dependent apoptosis in cisplatin-resistant ovarian cancer cells. *Mol Cancer Ther* **7**, 1410–1419.

[67] Haggarty SJ, Koeller KM, Wong JC, Grozinger CM, and Schreiber SL (2003). Domain-selective small-molecule inhibitor of histone deacetylase 6 (HDAC6)–mediated tubulin deacetylation. *Proc Natl Acad Sci USA* **100**, 4389–4394.

[68] Lee YS, Lim KH, Guo X, Kawaguchi Y, Gao Y, Barrientos T, Ordentlich P, Wang XF, Counter CM, and Yao TP (2008). The cytoplasmic deacetylase HDAC6 is required for efficient oncogenic tumorigenesis. *Cancer Res* **68**, 7561–7569.

Table W1. Randomization of Mice into Eight Separate Treatment Groups (n = 8 per Group) after Tumor Development to 100 mm^3.

Treatment Group	Intervention No. 1	Dose Interim No. 1	Route No. 1	Intervention No. 2	Dose Interim No. 2	Route No. 2
1	vehicle	24 hours	Oral	None	None	None
2	cisplatin 6 mg/kg	6 days	IP	None	None	None
3	OSU-HDAC42 25 mg/kg	24 hours	Oral	None	None	None
4	OSU-HDAC42 50 mg/kg	48 hours	Oral	None	None	None
5	SAHA 50 mg/kg	24 hours	Oral	None	None	None
6	OSU-HDAC42 25 mg/kg	24 hours	Oral	Cisplatin 6 mg/kg	6 days	IP
7	OSU-HDAC42 50 mg/kg	48 hours	Oral	Cisplatin 6 mg/kg	6 days	IP
8	SAHA 50 mg/kg	24 hours	Oral	Cisplatin 6 mg/kg	6 days	IP

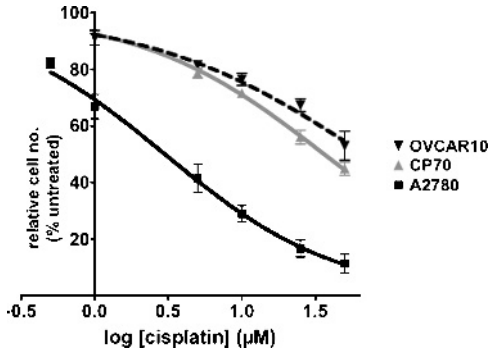

Figure W1. Forty-eight–hour cisplatin dose-response curves for OVCAR10, CP70, and A2780 cell lines, with respective IC_{50} values of 53.1, 42.6, and 3.2 μM. Means ± SE.

Table W2. Comparison of IC_{50} Values of OSU-HDAC42 and SAHA for Three Different Ovarian Cancer Cell Lines.

Cell Line	OSU-HDAC42 IC_{50} (μM)	SAHA IC_{50} (μM)	Significant at $P < .05$
A2780	0.39 ± 0.05	0.71 ± 0.07	Yes
Hey	1.40 ± 0.22	2.25 ± 0.5	Yes
HeyC2	1.85 ± 0.36	2.27 ± 0.30	No

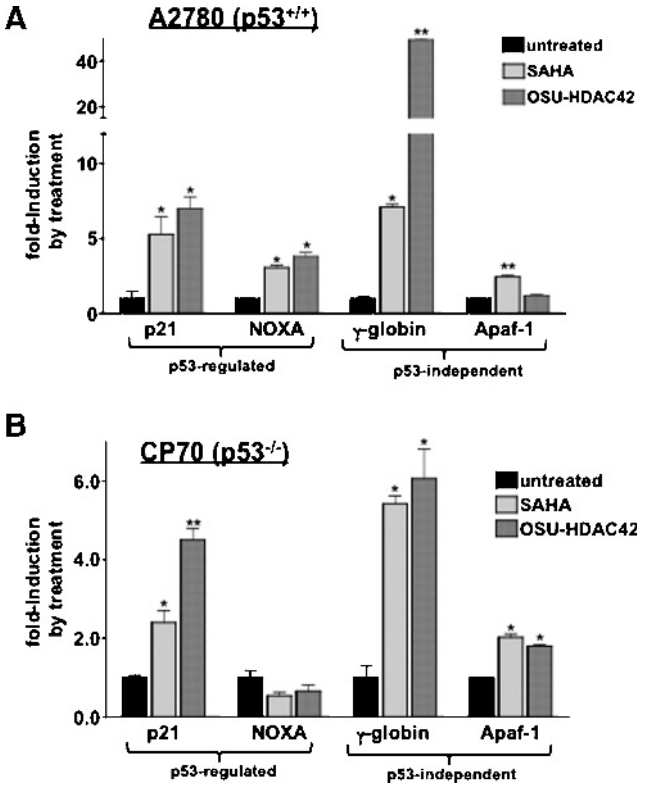

Figure W2. Quantitative PCR analysis of p53-regulated (*p21* and *NOXA*) and p53-independent (*γ-globin* and *Apaf1*) gene expression in (A) A2780 (p53-functional) and (B) CP70 (p53-dysfunctional) cells after a 24-hour treatment with vehicle or 1.0 μM OSU-HDAC42 or SAHA. Means $\pm$ SE. *$P < .05$, SAHA or OSU-HDAC42 *versus* untreated; **$P < .05$, SAHA *versus* OSU-HDAC42.

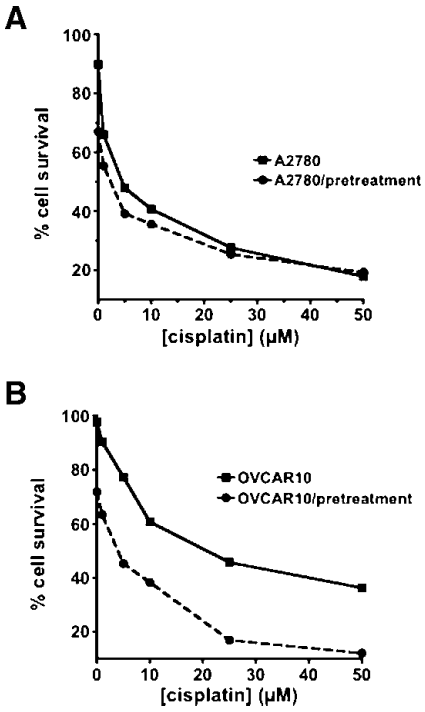

Figure W3. Forty-eight–hour cisplatin dose-dependent growth inhibition of (A) chemosensitive A2780 cells with or without 4 hours of 0.5 μM (the A2780 IC_{50} dose) OSU-HDAC42 pretreatment, or (B) chemoresistant OVCAR10 cells with or without 4-hour pretreatment with 1.0 μM (respective IC_{50} value) OSU-HDAC42.

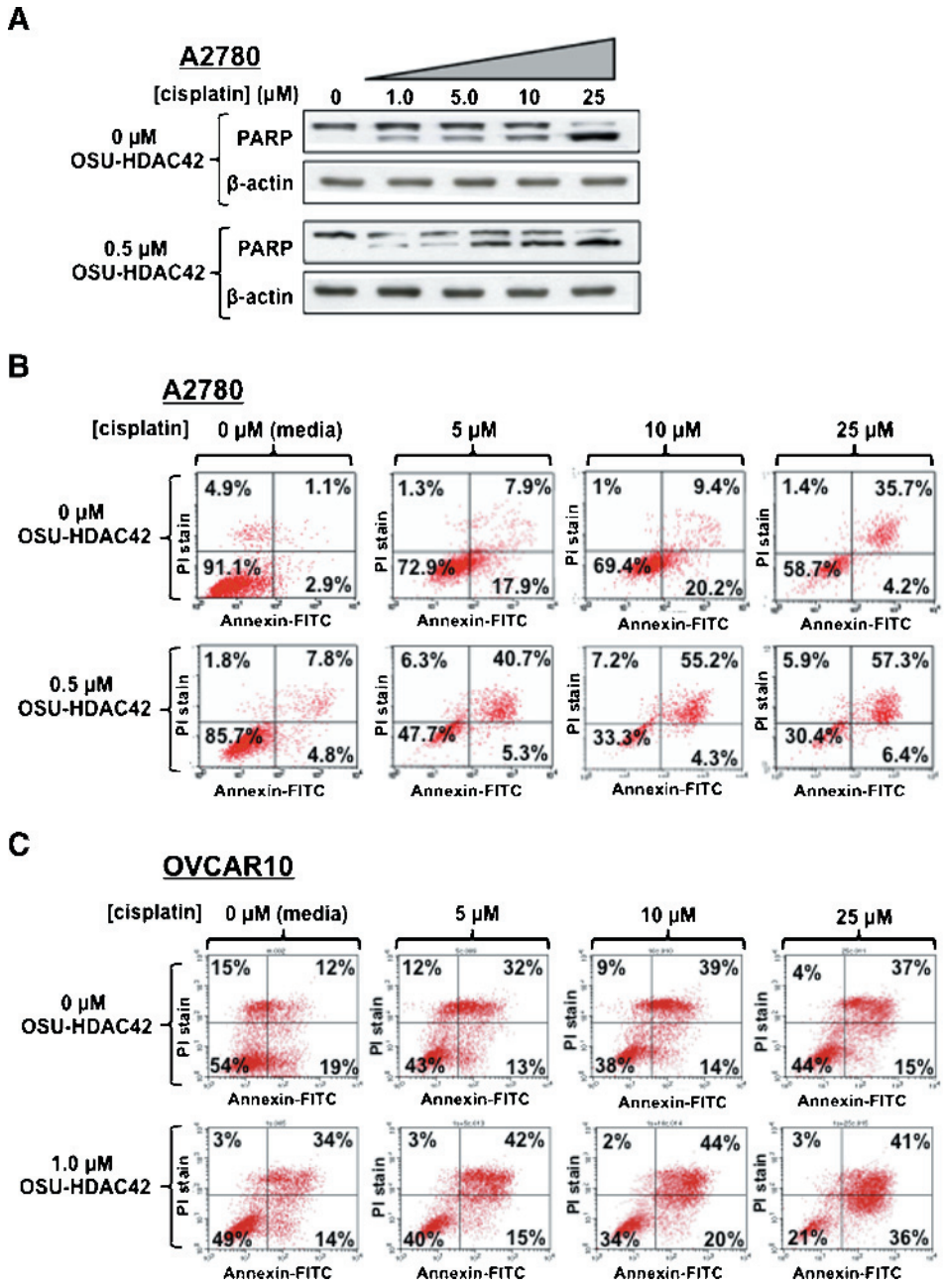

Figure W4. (A) Effects of a 4-hour 0.5 μM OSU-HDAC42 pretreatment of chemosensitive A2780 cells on 48-hour cisplatin dose-dependent, apoptosis-associated PARP cleavage or (B) annexin V–FITC binding to membrane-externalized phosphatidylserine (with PI used to measure total cell viability). (C) Identical annexin V–FITC assessment of OVCAR10 cells as in (B), except for pretreatment with 1.0 μM OSU-HDAC42.